

Available online at [www.sciencedirect.com](http://www.sciencedirect.com)**ScienceDirect**

Procedia CIRP 43 (2016) 64 – 69

[www.elsevier.com/locate/procedia](http://www.elsevier.com/locate/procedia)

14th CIRP Conference on Computer Aided Tolerancing (CAT)

## Tolerance analysis considering form errors in planar datum features

Antonio Armillotta\*

*Dipartimento di Meccanica, Politecnico di Milano, Via La Masa 1, 20156 Milano, Italy*\* Tel.: +39-02-23998296; fax: +39-02-23998585. E-mail address: [antonio.armillotta@polimi.it](mailto:antonio.armillotta@polimi.it)

### Abstract

The paper investigates the role of planar datum features in tolerance analysis problems. Mating relations between datum planes are shown to involve translational and rotational errors, which are related to form tolerances and are usually neglected in tolerance analysis. To evaluate these errors, the contact between datum planes was simulated by a stochastic model, where two surface profiles are randomly generated and then registered to reproduce a mating condition. Concepts of fractal geometry were exploited to make the generation consistent with the autocorrelation properties of actual surfaces resulting from manufacturing processes. A simulation plan allowed to predict the amount of contact errors as a function of size, tolerance and process-related assumptions on the two features. An example of 3D tolerance chain is presented to demonstrate the relevance of form errors in the variation of assembly requirements.

© 2016 The Authors. Published by Elsevier B.V. This is an open access article under the CC BY-NC-ND license

[\(http://creativecommons.org/licenses/by-nc-nd/4.0/\)](http://creativecommons.org/licenses/by-nc-nd/4.0/).

Peer-review under responsibility of the organizing committee of the 14th CIRP Conference on Computer Aided Tolerancing

*Keywords:* tolerance chain; GD&T; form tolerance; datum; fractal geometry; simulation.

### 1. Introduction

In tolerance analysis, the variation on an assembly-level geometric requirement is calculated as a stackup of errors on individual parts [1]. Input data include nominal part geometry, assembly structure, and tolerances specified on part features. Charting methods are available for this task when the stackup can be described by an explicit equation [2]. When solving three-dimensional problems, however, this cannot usually be done and mathematical procedures have been proposed to estimate the statistical distribution of the requirement [3]. These are based on representation models such as vector loops [4], small displacement torsors [5-7], transform chains [8, 9], Jacobian torsors [10], technologically and topologically related surfaces [11], virtual joints [12], and T-maps [13].

In order to comply with the whole set of ISO/ASME geometric tolerances, the above methods include criteria to decide which types of geometric control are relevant to any given assembly requirement. A common rule is to neglect form tolerances except in special cases. This is reasonable when a feature is assigned orientation or location tolerances, thus making the contribution of each control hardly separable. A form tolerance, however, may be specified as the only control on a feature, as in the case of a plane selected as

primary datum for a part. Neglecting the flatness tolerance on such a feature is equivalent to assume that planar surfaces of different parts come into contact through their high-point planes. Deviations from this condition are believed to have a negligible impact on tolerance analysis.

This paper tries to further investigate the relevance of form tolerances and the way to consider them in tolerance analysis. Stochastic modeling is used to verify whether form errors cause significant deviations from the nominal contact relation between planar datums. The same methodology has been widely used in variational geometry methods [14], which analyze error stackups on random surface models (rather than assuming rigid transformations on nominal features). They allow potential advantages such as the modeling of additional types of errors (e.g. profile and location), the consideration of complex-shaped features or compliant parts, the simultaneous treatment of systematic and random errors, and the integration with inspection data for the generation of random features. Recent methods of this type include skin model shapes [15], statistical modal analysis [16], mode shapes [17], and morphing meshes [18].

In this paper, concepts of fractal geometry are used to relate the simulation procedure with the topography of surfaces obtained by different manufacturing processes. As suggested

in [19-22], fractal methods synthesize the autocorrelation properties of surfaces in a limited number of parameters, yet allowing the generation of complex, realistic profiles [23].

## 2. Problem definition and approach

Any assembly requirement corresponds to a tolerance chain, i.e. a sequence of geometric relations between features of individual parts. A mathematical model of the chain is needed to express the requirement as a function of geometric attributes of the features. The following reasoning will be based on the transform chain model described in [24].

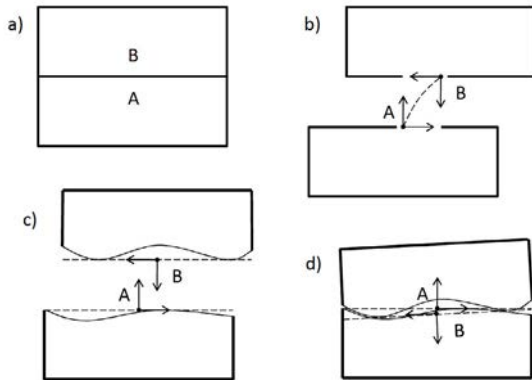


Fig. 1. Definition of contact errors: (a) planar contact; (b) nominal transformation; (c) flatness errors; (d) actual transformation.

Consider a mating relation between two planes A and B within a tolerance chain (Fig. 1a). If a coordinate frame is associated to each feature, the relation is described by a nominal transform matrix  $\mathbf{T}_{AB}$  between the two frames, which depends on nominal part geometry (Fig. 1b). The tolerance chain is thus described as a product of matrices including  $\mathbf{T}_{AB}$ . It is usually assumed that the transform chain does not change in the presence of flatness errors on the two features. If both planes are datums for the respective parts, this means that the high-point planes of the features coincide as a result of the mating (Fig. 1c). However, flatness errors can cause small translational and rotational displacements between the two high-point planes, which will be referred to as contact errors (Fig. 1d). The actual transform thus becomes

$$\mathbf{T}'_{AB} = \mathbf{T}_{AB} \cdot \mathbf{DT}_{AB}$$

where the elements of the error transform matrix  $\mathbf{DT}_{AB}$  are random variables that depend on the flatness tolerances of the two planes. Quantifying the contact errors (i.e. estimating the distributions of the elements of  $\mathbf{DT}_{AB}$ ) can help to verify whether they are to be neglected or can actually have an impact on tolerance chains in practical cases.

A way to estimate the contact errors is to simulate the mating relation between random surface profiles consistent with the flatness tolerances. To this end, a basic consideration is that any engineering surface is autocorrelated, i.e. the expected height difference of the profile in any two points

decreases with the distance of the points. Profile height can thus be decomposed into sinusoidal signals, whose amplitudes decrease with increasing frequency. Such a profile could be randomly generated by an inverse Fourier transform from statistical assumptions on the amplitudes for given manufacturing processes and parameters. Unfortunately, such assumptions are difficult to make in general cases.

Fractal geometry helps to reduce the complexity of the stochastic process needed to generate the profiles. For a fractal signal  $z(x, y)$  in two spatial variables, the expected height differences  $\Delta z$  are related to the differences  $\Delta x$  and  $\Delta y$  in the abscissas by the following power law:

$$\Delta z \propto \Delta s^H, \quad s = \sqrt{\Delta x^2 + \Delta y^2}, \quad 0 \leq H \leq 1 \quad (1)$$

where the parameter  $H$  is related to the degree of autocorrelation, e.g.  $H = 0$  for white noise,  $H = 0.5$  for Brownian motion,  $H = 1$  for analytic surfaces. The Fourier analysis of such a signal reveals that the spectral density  $|F(f)|^2$  (squared modulus of the complex amplitude) decreases with frequency  $f$  according to a power  $\beta$  related to  $H$ :

$$|F(f)|^2 \propto \frac{1}{f^\beta}, \quad \beta = 2H + 2 \quad (2)$$

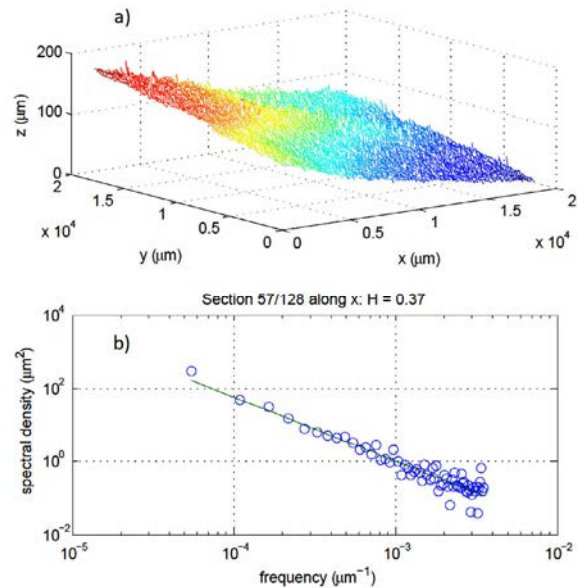


Fig. 2. Fractal analysis of a die-cast surface: (a) profile; (b) frequency spectrum for a cross-section.

This property helps to estimate  $H$  from samples of the signal. Many engineering surfaces have been shown to have fractal properties, i.e. they can be described by a single parameter without the need of evaluating the individual components of the Fourier spectrum. As an example, the topography of a  $20 \times 20$  mm planar region on a die-cast part has been collected by an Alicona InfiniteFocus profilometer with a  $7 \mu\text{m}$  resolution, and later subsampled on a grid of 128

$\times 128$  points (Fig. 2a). The Fourier analysis of profile sections (Fig. 2b) shows a decreasing trend of spectral density with frequency, with values of  $H$  between 0.35 and 0.45 (equivalent to  $\beta = 1.7-1.9$ ). As a comparison, values of  $H$  between 0.5 and 0.8 are reported in literature for machined surfaces.

From the above considerations, the proposed approach to the evaluation of contact errors consists in the following steps:

- identify the contact errors and define the elements of the error transform matrix associated to a mating relation;
- find statistical distributions for the contact errors by simulating the mating of planes with given size, tolerances and fractal properties (parameter  $H$ );
- analyze the sensitivity of the above distributions with respect to the properties specified for the features;
- provide a criterion to quantify the contact errors in a tolerance analysis problem.

### 3. Simulation of contact errors

Consider the contact between two nominally planar profiles  $z_1(x, y)$  and  $z_2(x, y)$  with size  $L \times L$ , assuming that both are datum features for the respective parts. Due to flatness errors  $E_1$  and  $E_2$  on the two features, the high-point planes of the two profiles do not coincide. Let the frame associated to each feature have the  $x$  and  $y$  axes on the high-point plane and the  $z$  axis perpendicular to the same plane towards the outside (as in Fig. 1). After linearization, the actual transform between the two frames is given by

$$\mathbf{T}'_{1-2} = \mathbf{T}_{1-2} \cdot \mathbf{DT}_{1-2} = \begin{bmatrix} -1 & 0 & 0 & 0 \\ 0 & -1 & 0 & 0 \\ 0 & 0 & -1 & 0 \\ 0 & 0 & 0 & 1 \end{bmatrix} \begin{bmatrix} 1 & 0 & \delta\theta_y & 0 \\ 0 & 1 & -\delta\theta_x & 0 \\ -\delta\theta_y & \delta\theta_x & 1 & \delta\tilde{x} \\ 0 & 0 & 0 & 1 \end{bmatrix}$$

where  $\delta\tilde{x}$  (small translation along  $z$ ),  $\delta\theta_x$  and  $\delta\theta_y$  (small rotations about  $x$  and  $y$ ) are the contact errors. To estimate their statistical distributions, each profile will be assumed to have fractal properties with given  $H$ . Instances of the profile can be generated by the method of successive random additions. An initial profile is built by applying random displacements along  $z$  to the vertices of the square planar area; height differences are extracted from a normal distribution with zero mean and standard deviation  $\sigma_0$  consistent with a given flatness tolerance. The profile is then recursively divided into equal square pieces, whose vertices are also randomly displaced along  $z$ . The distances are extracted from normal distributions whose standard deviations decrease at each recursion level  $i$  according to the following equation:

$$\sigma_i = \frac{\sigma_0}{2^{iH/2}}, \quad i = 1, \dots, n$$

thus eventually obtaining a profile with  $(2^n + 1)$  points along  $x$  and  $y$ . Different values of  $H$  result in profiles with different appearances, where the contribution of higher-frequency components decreases with increasing  $H$ .

The above procedure is the basis for the simulation of mating profiles. Two random profiles are first translated along  $z$  and rotated about  $x$  and  $y$  so as to minimize the average vertical distance to a same horizontal plane, subject to a constraint of zero minimum distance; this leads the high-point planes of the two profiles to coincide (the usual assumption in tolerance analysis). The distances to the common plane allow to evaluate the two flatness errors and can be displayed appropriately, e.g. by contour plots (Fig. 3).

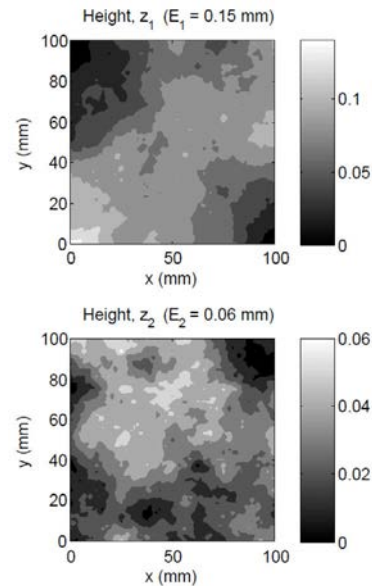


Fig. 3. Example of three-dimensional profiles ( $H = 0.6$ ).

Keeping then fixed the lower profile  $z_1$ , the upper profile  $z_2$  is translated and rotated so as to minimize the average vertical distance between the two profiles (or, equivalently, the vertical distance between the centers of mass of the two profiles), subject to a constraint of zero minimum distance; this requires a new rigid transform given by the three contact errors  $\delta\tilde{x}$ ,  $\delta\theta_x$  e  $\delta\theta_y$  (Fig. 4a). This is equivalent to letting the two profiles touch at three actual contact points, as clearly visible in the display of the final gap  $z_2 - z_1$  (Fig. 4b).

The distributions of the three random variables are estimated by repeating the procedure for a large number of instances of the two profiles. A few properties can be easily predicted:  $\delta\tilde{x}$  takes only negative values because the upper profile moves down approaching the lower one;  $\delta\theta_x$  and  $\delta\theta_y$  are expected to have zero mean and equal standard deviations due to symmetry (Fig. 5).

### 4. Analysis of influence factors

The simulation procedure can help to observe how the distributions of contact errors depend on design specifications. Four factors are expected to influence the interaction between the profiles of mating planes. The parameter  $H$  represents the topographic properties of features resulting from a given manufacturing process, while the size  $L$  and the flatness tolerances  $T_1$  and  $T_2$  determine the dimensions of the profiles.

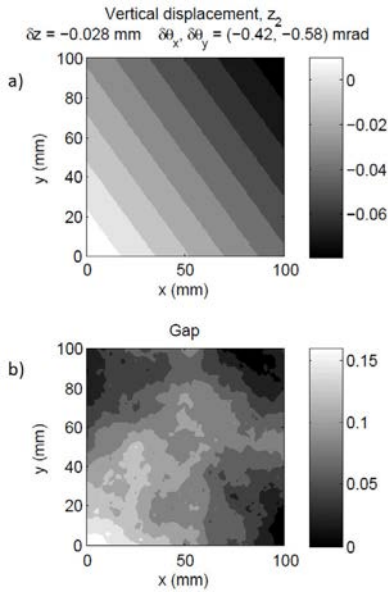


Fig. 4. Contact errors on three-dimensional profiles: (a) displacement map of the upper profile; (b) resulting gap.

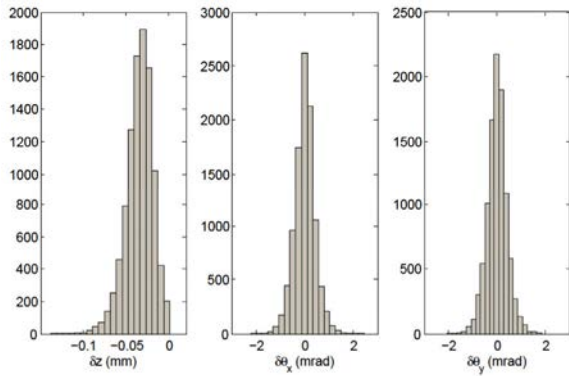


Fig. 5. Distributions of contact errors ( $L = 100$  mm,  $H = 0.6$ ,  $T_1 = T_2 = 0.2$  mm, 10,000 runs).

Two initial considerations help to predict the influence of the above factors. First, if one of the tolerances were equal to zero, the corresponding profile would coincide with its high-point plane; therefore, the other profile could not change its position further as a result of the contact. It is thus expected that the contact errors increase with the minimum  $T_{\min}$  of the two tolerances. Secondly, the rotational errors are expected to be inversely proportional to the size  $L$  of the features for given tolerances. As a result, the following dimensionless variables are defined for the contact errors:

$$\delta z' = \frac{\delta z}{T_{\min}}, \delta \theta'_x = \frac{\delta \theta_x}{T_{\min}/L}, \delta \theta'_y = \frac{\delta \theta_y}{T_{\min}/L} \quad (3)$$

A  $2^4$  full factorial plan of these three responses has been conducted with the levels listed in Tab. 1 and 200 simulation runs for each treatment. A preliminary analysis of the results

confirms that  $\delta z'$  has a skewed distribution of negative values, while  $\delta \theta'_x$  and  $\delta \theta'_y$  have symmetric distributions with means close to zero and nearly equal standard deviations (although they fail the appropriate statistical tests on the whole sample). The results have been further analyzed to evaluate the effects of the factors on the sample mean of  $\delta z'$  and on the sample standard deviations of  $\delta \theta'_x$  and  $\delta \theta'_y$ .

Tab. 1. Factorial plan of simulations.

Factor	Levels
$H$	0.4, 0.8
$L$ (mm)	50, 100
$T_1$ (mm)	0.2, 0.4
$T_2$ (mm)	0.2, 0.4

As regards the individual effects, it results that  $L$  does neither significantly influence the parameters of  $\delta z'$  (e.g. for the mean: t-test with  $p = 0.42$ , Levene's test with  $p = 0.66$ ), nor the standard deviations of  $\delta \theta'_x$  and  $\delta \theta'_y$  (F-tests with  $p = 0.27$  and  $0.94$ ). This suggests that the effect of feature size is completely accounted for by the definition of the two dimensionless angular errors in (3).

Differently,  $H$  has significant effects on the mean and standard deviation of  $\delta z'$  (t-test and Levene's test with  $p \approx 0$ ) as well as on the standard deviations of  $\delta \theta'_x$  and  $\delta \theta'_y$  (both F-tests with  $p \approx 0$ ). Contact errors are thus likely to depend on the manufacturing processes of the mating parts.

The analysis also shows an interaction between  $T_1$  and  $T_2$ , as larger errors arise when the two features have different tolerances. This suggests that, beside the effect of  $T_{\min}$  already considered in the dimensionless variables, an additional influence factor  $|T_2 - T_1|$  is to be considered. Actually, the difference of the two tolerances significantly influences the mean and the standard deviation of  $\delta z'$  (t-test and Levene's test with  $p \approx 0$ ) as well as the standard deviations of  $\delta \theta'_x$  and  $\delta \theta'_y$  (both F-tests with  $p \approx 0$ ). The main statistics of the three error components as a function of the two influence factors (Tab. 2) show that  $|T_2 - T_1|$  has a weaker effect than  $H$ .

Tab. 2. Statistics of the contact errors from the simulation plan.

$H$	$ T_1 - T_2 $ (mm)	$\delta z'$ , mean	$\delta \theta'_x$ , st. dev.	$\delta \theta'_y$ , st. dev.
0.8	0	-0.132	0.171	0.171
	0.2	-0.169	0.213	0.221
0.4	0	-0.261	0.267	0.276
	0.2	-0.334	0.358	0.391

### 5. Application to tolerance analysis

The results of the simulation plan lead to a first-approximation criterion for the random generation of contact errors within a tolerance analysis model. The three error components can be extracted from normal distributions with the following parameters (mean and standard deviation):

$$\delta z: \mu = -kT_{\min}, \sigma = kT_{\min}/3 \quad (4)$$

$$\delta\theta_x, \delta\theta_y : \mu=0, \sigma=kT_{\min}/L \tag{5}$$

where  $k$  is a dimensionless constant. As an improvement to the usual practice of neglecting contact errors ( $k = 0$ ), suitable values can be selected for  $k$  according to the results in Tab. 2. Specifically,  $k = 0.15$  would be appropriate for surfaces with equal tolerances obtained by accurate machining ( $H \approx 0.8$ ). For non-machined surfaces (e.g. die cast as in the previous example,  $H \approx 0.4$ ) with highly different tolerances,  $k = 0.30$  could be a better choice. Intermediate values of the constant could be selected in different cases.

The criterion is intentionally simple and has two main shortcomings. First, the constant  $k$  is only qualitatively related to the influence factors highlighted in the simulation. Secondly, a normal distribution is assumed for the translational error  $\delta X$  instead of skewed distributions (e.g. exponential) suggested in literature for zero-limited geometric errors [25]; in a tolerance analysis problem with many random variables, this choice should not involve significant distortions due to the central limit theorem.

As an application example, consider a simple assembly where the clearance  $X$  between two pins connected to a plate is to be accurately controlled (Fig. 6a). Geometric tolerances according to ISO standards are specified on the two parts (Fig. 6b, showing only dimensions relevant to the problem).

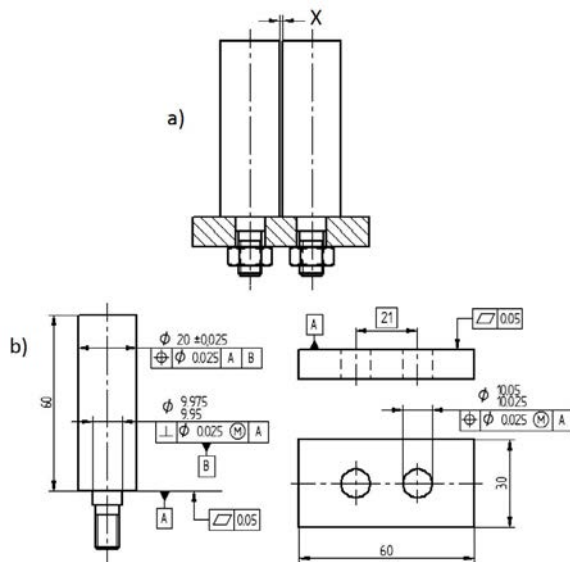


Fig. 6. Example: (a) assembly; (b) toleranced parts.

The distribution of the requirement  $X$  is estimated by the transform chain method. Frames with equal orientation are associated to all the assembly features and to two opposed points with distance  $X$  (Fig. 7a). Some frames have also translated and/or rotated configurations due to the geometric errors allowed by the tolerances. Considering all the frames in the correct order (Fig. 7b), the chain of frames associated to  $X$  is described by the following matrix product:

$$\mathbf{T}_{1-8} = \mathbf{DT}_1 \cdot \mathbf{T}_{1-2} \cdot \mathbf{DT}_2 \cdot \mathbf{T}_{2-3} \cdot \mathbf{T}_{3-4} \cdot \mathbf{DT}_{3-4} \cdot \mathbf{T}_{4-5} \cdot \mathbf{DT}_5 \cdot \mathbf{T}_{5-6} \cdot \mathbf{DT}_{5-6} \cdot \mathbf{T}_{6-7} \cdot \mathbf{DT}_7 \cdot \mathbf{T}_{7-8} \cdot \mathbf{DT}_8 \tag{6}$$

whose element corresponding to the translation along  $y$  (second row, fourth column) gives  $X$ .

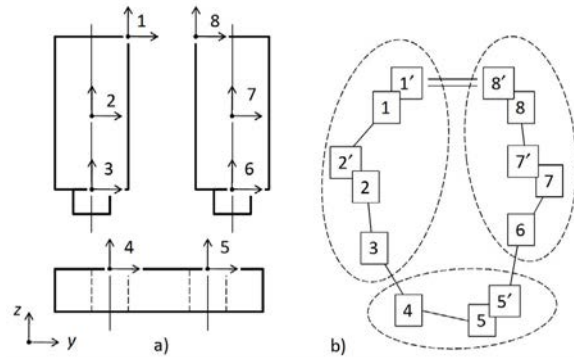


Fig. 7. Tolerance analysis model: (a) frames associated to the features; (b) transform chain.

In the common approach, the matrices are evaluated without considering the contact errors as detailed in Appendix A. The proposed criterion completes the matrices  $\mathbf{DT}_{3-4}$  and  $\mathbf{DT}_{5-6}$  with additional error components according to equations (4-5), where  $T_{\min}$  is the flatness tolerance on the primary datum of the pin (0.05 mm) and  $L$  is the nominal diameter of the pin (20 mm). Assuming  $k = 0.15$  and performing a Monte Carlo simulation with 10,000 runs yields the distribution of  $X$  (Fig. 8a). The comparison with the distribution found without the contact errors ( $k = 0$ ) shows a clear increase of the  $\pm 3\sigma$  tolerance on the requirement (Fig. 8b).

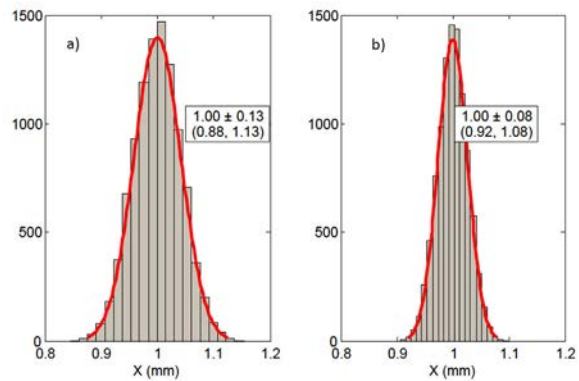


Fig. 8. Distribution of the assembly requirement: (a) with contact errors; (b) without contact errors.

## 6. Conclusions

Form errors are usually neglected in tolerance analysis. The paper has proposed a criterion to estimate their effects when a tolerance chain includes mating datum planes. In these cases, translational and rotational error components can be randomly generated from normal distributions with appropriate parameters. These are suggested according to the results of a

simulation plan which evaluates the effects of design specifications on the contact errors.

The application example shows that the effects of form errors may actually be relevant in special cases. These include tolerance chains with contacts between small-sized datum planes obtained by manufacturing processes with limited accuracy and possibly different for the mating features.

The limitations of the proposed criterion include the lack of experimental validation, the selection of a single type of stochastic model of surface profiles, and the reference to a single tolerance analysis method. It also neglects some secondary effects which might further increase the contact errors, such as the deformations due to contact stresses. Future studies will try to address these issues.

## Appendix A. Tolerance analysis model

The matrices in (5) have the following structures:

$$\mathbf{T}_{i-j} = \begin{bmatrix} 1 & 0 & 0 & p_x \\ 0 & 1 & 0 & p_y \\ 0 & 0 & 1 & p_z \\ 0 & 0 & 0 & 1 \end{bmatrix}, \quad \mathbf{DT}_{i-j} = \begin{bmatrix} 1 & -\delta\theta_z & \delta\theta_y & \delta x \\ \delta\theta_z & 1 & -\delta\theta_x & \delta y \\ -\delta\theta_y & \delta\theta_x & 1 & \delta z \\ 0 & 0 & 0 & 1 \end{bmatrix}$$

In the nominal transforms  $\mathbf{T}_{i,j}$ , the rotation sub-matrices are identities because all the frames have the same orientation (Fig. 9a), while the translation vectors depend on the nominal dimensions of part features (Tab. A.1). In the error transforms  $\mathbf{DT}_{i,j}$ , selected elements are normally distributed with zero means and standard deviations depending on the tolerances (Tab. A.2), while the remaining elements equal zero.

Tab. A.1. Translation vectors of nominal transforms.

Matrix	$p_x$	$p_y$	$p_z$
$\mathbf{T}_{1-2}$	0	-20 / 2	-60 / 2
$\mathbf{T}_{2-3}$	0	0	-60 / 2
$\mathbf{T}_{3-4}$	0	0	0
$\mathbf{T}_{4-5}$	0	21	0
$\mathbf{T}_{5-6}$	0	0	0
$\mathbf{T}_{6-7}$	0	0	60 / 2
$\mathbf{T}_{7-8}$	0	-20 / 2	60 / 2

Tab. A.2. Standard deviations of nonzero elements of error transforms.

Matrices	Elements	Standard deviation
$\mathbf{DT}_1, \mathbf{DT}_8$	$\delta y$	0.025 / 6
$\mathbf{DT}_2, \mathbf{DT}_7$	$\delta x, \delta y$	0.025 / 6
	$\delta\theta_x, \delta\theta_y$	0.025 / 60
$\mathbf{DT}_{3-4}$	$\delta x, \delta y$	(0.05 + 0.05) / 6
$\mathbf{DT}_5$	$\delta y$	0.05 / 6

## References

- [1] Bjørke Ø. Computer-aided tolerancing. New York: ASME Press; 1989.
- [2] Fischer BR. Mechanical tolerance stackup and analysis. New York: Marcel Dekker; 2004.

- [3] Polini W. Geometric tolerance analysis. In: Colosimo B, Senin N, editors. Geometric tolerances. London: Springer; 2011. p. 39-68.
- [4] Chase KW, Magleby SP, Glancy CG. A comprehensive system for computer-aided analysis of 2-D and 3-D mechanical assemblies. Proc Int Sem Computer-Aided Tolerancing 1997, Toronto.
- [5] Giordano M, Hernandez P, Denimal D. Synthesis and statistical analysis for three-dimensional tolerancing. Proc Int Conf Computer-Aided Tolerancing 2009, Annecy.
- [6] Legoff O, Villeneuve F, Bourdet P. Geometric tolerancing in process planning: a tridimensional approach. Proc IMechE Part B 1999; 213:635-40.
- [7] Teissandier D, Couétard Y, Gérard A. A computer aided tolerancing model: proportioned assembly clearance volume. Comput Aided Des 1999; 31:805-17.
- [8] Whitney DE, Gilbert OL. Representation of geometric variations using matrix transforms for statistical tolerance analysis in assemblies. Res Eng Des 1994; 6:191-210.
- [9] Mantripragada R, Whitney DE. Modeling and controlling variation propagation in mechanical assemblies using state transition models. IEEE Trans Rob Autom 1999; 15-1:124-40.
- [10] Desrochers A, Ghie W, Laperrière. Application of a unified Jacobian-torsor model for tolerance analysis. J Comput Inf Sci Eng 2003; 3:2-14.
- [11] Salomons OW, Haalboom FJ, Jonge Poerink HJ, van Slooten F, van Houten FJAM, Kals HJJ. A computer-aided tolerancing tool II: tolerance analysis. Comput Ind 1996; 31:175-86.
- [12] Lafond P, Laperrière L. Jacobian-based modeling of dispersions affecting pre-defined requirements of mechanical assemblies. Proc IEEE Int Symp Assembly and Task Planning 1999, Porto.
- [13] Shen Z, Ameta G, Shah JJ, Davidson JK. A comparative study of tolerance analysis methods. J Comput Inf Sci Eng 2005; 5:247-56.
- [14] Gupta S, Turner JU. Variational solid modeling for tolerance analysis. IEEE Comput Graph App 1993; 13-3:64-74.
- [15] Schleich B, Anwer N, Mathieu L, Wartzack S. Skin model shapes: a new paradigm shift for geometric variations modelling in mechanical engineering. Comput Aided Des 2014; 50:1-15.
- [16] Huang W, Kong Z. Simulation and integration of geometric and rigid body kinematic errors for assembly variation analysis. J Manuf Sys 2008; 27:36-44.
- [17] Samper S, Adragna PA, Favreliere H, Pillet M. Modeling of 2D and 3D assemblies taking into account form errors of plane surfaces. J Comput Inf Sci Eng 2009; 9:041005/1-12.
- [18] Franciosa P, Gerbino S, Patalano S. Simulation of variational compliant assemblies with shape errors based on morphing mesh approach. Int J Adv Manuf Technol 2011; 53:47-61.
- [19] Ganti S, Bhushan B. Generalized fractal analysis and its applications to engineering surfaces. Wear 1995; 180:17-34.
- [20] Hasegawa M, Liu J, Okuda K, Nunobiki M. Calculation of the fractal dimensions of machined surface profiles. Wear 1996; 192:40-5.
- [21] Russ JC. Fractal dimension measurement of engineering surfaces. Int J Mach Tools Manuf 1998; 38:567-71.
- [22] Jiang Z, Wang H, Fei B. Research into the application of fractal geometry in characterising machined surfaces. Int J Mach Tools Manuf 2001; 41:2179-85.
- [23] Peitgen HO, Saupe D. The science of fractal images. New York: Springer; 1988.
- [24] Whitney DE. Mechanical assemblies. New York: Oxford University Press; 2004.
- [25] Braun PR, Morse EP, Voelcker HB. Research in statistical tolerancing: examples of intrinsic non-normalities and their effects. Proc. Int. Sem Computer-Aided Tolerancing 1997, Toronto.